Journal of Science and Engineering Papers
Volume: 02, Issue: 01 (January), 2025, page: 96-100
Journal homepage: www.jsciengpap.com
https://doi.org/10.62275/josep.24.1000001

*ISSN: 3006-3191 (online)*

# Biosynthesis of zero-dimensional $TiO_2$ nanostructures for potential photocatalytic applications

**Raiyana Mashfiqua Mahmud[1], Abdullah Al Moyeen[1,] *, Abdul Al Mamun[2], Md. Khairul Islam[1], Md. Lael Hasan[1], and Md. Estabrak Ahammod Sakib[1]**

[1]Dept. of Glass & Ceramic Engineering, Rajshahi University of Engineering & Technology, Rajshahi-6204, Bangladesh.
[2]Dept. of Materials Science & Engineering, Rajshahi University of Engineering & Technology, Rajshahi-6204, Bangladesh.

*Corresponding author: e-mail address: abdullah264253@gmail.com; ORCID: https://orcid.org/0009-0002-7018-0249



**ARTICLE INFO**

**Received: 30th September, 2024**
**Revised: 6th November, 2024**
**Accepted: 12th November, 2024**

***Keywords:***

biosynthesis
anatase $TiO_2$
bandgap
methylene blue
photocatalytic activity

**ABSTRACT**

This study introduces a sustainable approach to synthesize zero-dimensional $TiO_2$ nanostructures using *Allium sativum* (garlic) clove extract as a biogenic capping and reducing agent. The synthesized particles were dried at 80 ºC for 24 hours and calcined at 450 ºC for 2 hours. X-ray diffractometer (XRD), Field Emission Scanning Electron Microscopy (FESEM), UV-vis spectroscopy, and photocatalytic activity analysis were used to characterize the synthesized nanoparticles. The XRD pattern revealed the prevalence of the tetragonal anatase phase in the synthesized nanostructures, with an average crystallite size of 6.45 nm. The Williamson-Hall plot method was employed to evaluate the type of strain induced in the synthesized particles, and the crystallinity of $TiO_2$ nanostructures was estimated to be 74.91%. The Rietveld analysis calculated the lattice parameters, cell volume, and other relevant parameters. FESEM image showed spherical nanostructures with an average size of 45.08 nm. UV-vis spectroscopy indicated an optically active region at ~361 nm, and the direct bandgap, calculated using the Tauc plot, was 3.28 eV. The photocatalytic efficiency of $TiO_2$ for methylene blue degradation reached 86.23% within 90 minutes, showing its potential for environmental remediation.

## 1. Introduction

Zero-dimensional $TiO_2$ nanostructures, commonly referred to as $TiO_2$ nanoparticles (NPs), are a class of transition metal oxide semiconductors that have garnered considerable attention in materials science research. These nanostructures are nanoscale particles with high surface-area-to-volume ratios and special quantum confinement effects because they are restricted in all three dimensions, unlike one-dimensional (nanotubes) or two-dimensional (nanosheets) structures. Their high potential for diverse applications, particularly in solar energy conversion and environmental remediation, highlights their importance in contemporary research [1]. Physically, rutile, anatase, and brookite are the three polymorphic phases of $TiO_2$. Whereas brookite has an orthorhombic structure, anatase and rutile adopt a tetragonal shape. In practical terms, the anatase $TiO_2$ has greater photocatalytic activity than the rutile and brookite phases. With its large specific surface area and modest quantum confinement, well-crystallized anatase $TiO_2$ with small particle size can improve photocatalytic performance by increasing the number of active surface sites and decreasing the distance required for interface migration [2]. Synthesizing $TiO_2$ NPs, which have morphologies and regulated crystal phases that make them highly appropriate for a variety of high-performance applications, has consistently proven to be an intrinsically complex and demanding endeavor for the scientific community [3].

As a transition metal oxide and perfect semiconducting material, $TiO_2$ offers special qualities such as reduced cost, low toxicity, ease of handling, and resistance to both chemical and photochemical degradation. Electronically, $TiO_2$ has a wide band gap that enables it to absorb UV light and generate electron-hole pairs, which can drive oxidation and reduction reactions, a property crucial for applications in photocatalysis, solar energy conversion, and environmental remediation. Because of its high surface area, high capacity for molecular oxygen adsorption, along with suppressed electron-hole pair recombination, it has a high catalytic activity [4]. $TiO_2$ has numerous benefits, including strong antibacterial properties, self-cleaning capabilities, and biocompatibility. Due to these

remarkable attributes, nanocrystalline $TiO_2$ exhibits a wide range of potential applications, including gas sensors, fillers, biomaterials, dielectric materials, pigments, catalyst supports, solar cells, coatings, environmental purification, and hydrogen gas production. The textile industry generates a significant amount of hazardous and non-biodegradable color dye effluents. By releasing hazardous and possibly cancer-causing chemicals into the aqueous phase, these colors seriously contaminate the environment [5]. The advancement of efficient and eco-friendly methods for treating these effluents is crucial, and $TiO_2$ NPs, with their strong photocatalytic properties, hold great promise for degrading these persistent organic pollutants.

In the past few decades, numerous synthesis techniques have been developed and are extensively employed for the synthesis of $TiO_2$ nanostructures. These include green synthesis, the sol-gel route, hydrothermal technique, electro-deposition method, solvothermal synthesis, chemical vapor deposition technique, and direct oxidation method. Challenges in the biosynthesis of zero-dimensional $TiO_2$ nanostructures include the control of particle size and uniformity, their morphology, and crystallinity. Researchers can address these by optimizing synthesis parameters, using purified bioagents, and implementing mild thermal treatments. However, the eradication of the harmful effects brought on by numerous chemical processes has led to broad acceptance for the green synthesis [6]. In earlier research, $TiO_2$ nanoparticles were synthesized through green synthesis using various plant extracts, including the peel of *Citrus reticulata* (orange), the hydrated extract of *Curcuma longa* (turmeric), the aqueous leaf extract of *Azadirachta indica* (neem), the leaf extract of *Murraya koenigii* (Curry leaves tree), and the leaf extract of *Jatropha curcus L.* [4]. However, there are no reports available on the fabrication of $TiO_2$ nanostructures using garlic clove extract. The effect of garlic clove extract on silver and selenium nanoparticles is remarkable [7, 8]. Given the remarkable efficacy of garlic clove extract in producing silver and selenium nanoparticles, it is hypothesized that this natural resource could serve as a promising precursor for synthesizing $TiO_2$ nanoparticles with enhanced photocatalytic properties.

In this work, plant-derived compounds from garlic cloves were employed as a novel green alternative to chemically synthesized reagents for the synthesis of zero-dimensional $TiO_2$ nanostructures. Garlic clove extract served as both a reducing and capping agent, controlling the nanoparticles' size and preventing agglomeration. The main objective of this study was to comprehensively characterize the biosynthesized $TiO_2$ NPs in terms of their structural, morphological, optical, and photocatalytic properties.

## 2. Materials and methods

### *2.1. Synthesis of $TiO_2$ NPs*

Initially, garlic cloves were gathered, peeled, and thoroughly cleaned with deionized and tap water to remove surface contaminants. The cloves were then finely chopped. The pieces were then combined with 100 mL of deionized water to create the extract that was going to be utilized as a stabilizing agent. In order to facilitate the effective extraction of bioactive components from the pieces, this mixture was heated for 25 minutes at 100 °C. Subsequently, the extracts were cooled to ambient temperature before being filtered through Whatman No. 1 qualitative filter paper to get rid of any remaining pieces of solid contaminants. The resulting filtrate, containing the garlic clove extract, was refrigerated at 4 °C for future use.

For the production of $TiO_2$ nanoparticles, a solution of titanium isopropoxide (TTIP) at a concentration of 0.1 M was made. Then, 80 mL of deionized water was employed to dissolve this solution. Then, 40 mL of extract from garlic clove was added to the mixture. After that, the mixture was magnetically agitated for 3 h at 600 rpm while a thermocouple was used to keep the temperature constant at 60 °C. A small amount of $NH_3$ was supplemented to regulate the pH of the mixture. The produced solution was then aged for 24 h and maintained for gelation. After that, ethanol and deionized water were used to centrifuge and clean the reaction mixture. The $TiO_2$ NPs were then dried at 80 °C in a hot air oven for an entire night in order to remove any remaining moisture. After succeeding, the calcination was performed for 2 h at 450 °C. The NPs were then preserved for additional characterization.

### *2.2. Characterization*

To find out the characteristics of the synthesized $TiO_2$ nanostructures, several experiments were conducted. The characterization involved the use of a SHIMADZU LabX XRD-6100 instrument with Cu Kα radiation at 1.5418 Å for powder XRD, with the diffraction angle range (2θ) adjusted between 20° and 80°. The XRD data was subjected to Rietveld refinement using the FullProf software. Using a JEOL JSM-7600F model, Field Emission Scanning Electron Microscopy was utilized to examine the particles' morphology. After that, the particle size distribution from the FESEM image was estimated using ImageJ software. With ethanol, the $TiO_2$ nanoparticles' optical properties were determined by a Shimadzu UV-2600i UV-vis spectrophotometer. The bandgap of the NPs was evaluated from the experimental curve and the absorption spectra is obtained between 300 and 800 nm in wavelength.

### *2.3. Photocatalytic performance test*

Under UV light at a wavelength of 450–800 nm and an intensity of 120 μW/cm$^2$, the degradation of MB was carried out to examine the photocatalytic activity of biosynthesized $TiO_2$ NPs. Initially, 5 gm of $TiO_2$ and weighed MB dye were combined. After being installed in complete darkness for 2h, the mixture was exposed to UV light. Next, the mixture's light absorption at various periods was measured. The following equation (Eqn. 1) was used to quantify the photo deterioration proficiency [6]:

$$\text{Degradation efficiency, } \eta = \frac{C_0 - C_1}{C_0} \times 100 \quad \textbf{(1)}$$

where, $C_0$ and $C_1$ correspond to the absorption of MB solution before and after the adding of $TiO_2$ nanoparticles as a function of time t (0, 30, 60 and 90 minutes).

## 3. Results and discussion

### *3.1. Microstructural characteristics*

Figure 1a displays the XRD pattern of $TiO_2$ nanostructures that were synthesized using biosynthesis method. The Bragg's reflection planes of (101), (004), (200), (105), (204), (116), and (215) are corresponding to the diffraction angle (2θ) at 25.35°, 37.90°, 48.01°, 54.65°, 62.69°, 68.86°, and 75.25°, respectively. The prominent (101) peak at 25.35° indicated the high crystallinity of the synthesized particles. The overall XRD pattern matched the tetragonal crystal structure of $TiO_2$ as referenced in JCPDS card number 89-4920. To further elucidate the structural parameters, Rietveld refinement was performed using FullProf software and a Pseudo-Voigt profile function (Figure 1b). The refined lattice parameters (a, b, c) and unit cell volume were determined. The goodness-of-fit

https://doi.org/10.62275/josep.25.1000014

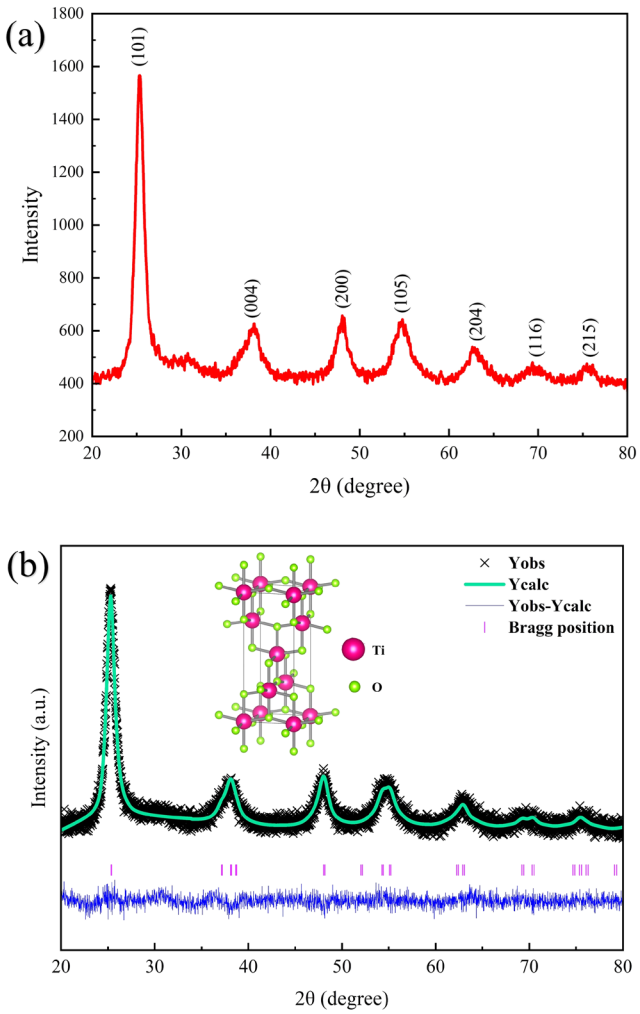


**Figure 1:** (a) XRD, and (b) Rietveld refined pattern of $TiO_2$ NPs.

indicators, including the weighted profile R-factor (Rwp), expected profile R-factor (Rexp), profile R-factor (Rp), and goodness-of-fit (GOF) values, were all below 10%, confirming the reliability of the Rietveld refinement results (Table 1). Additionally, based on the refined lattice parameters, the crystallographic structure was visualized using the VESTA software (inset of Figure 1b).

Using the Scherrer equation, the avg. crystallite size of the resulting $TiO_2$ nanostructures is calculated to be 6.45 nm. An

**Table 1:** Crystallographic parameters of $TiO_2$ NPs.

| **Crystallographic parameters** | | **$TiO_2$ NPs** |
|---|---|---|
| Lattice parameters | a = b | 3.7843 Å |
| | c | 9.4378 Å |
| Cell Volume | | 135.153 $Å^3$ |
| R-factors | $R_p$ | 4.43 |
| | $R_{wp}$ | 5.61 |
| | $R_{exp}$ | 4.55 |
| | Rf-factor | 1.17 |
| | Bragg R-factor | 2.41 |
| GOF | | 1.2 |
| X-ray density | | 4.353 $gcm^{-3}$ |
| FWHM | | 0.0216 |
| Crystallite size | For (101) plane | 6.45 nm |
| | Average (W-H plot) | 5.57 nm |
| Lattice strain | For (101) plane | 0.04900 |
| | Average (W-H plot) | 0.00408 |
| Crystallinity | | 74.91% |

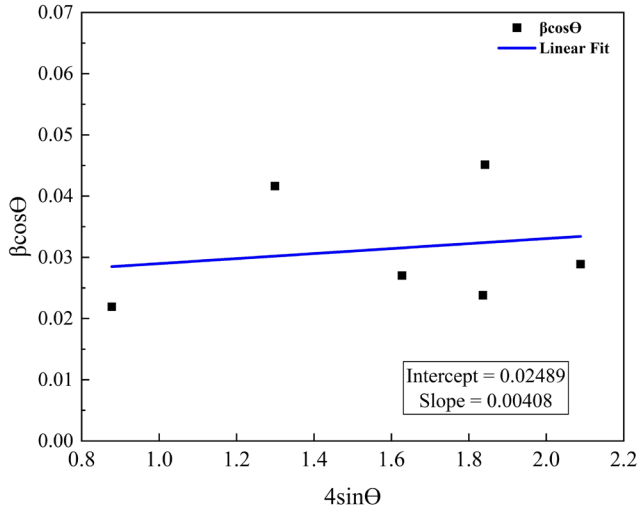


**Figure 2:** Williamson-Hall plot of $TiO_2$ NPs.

extended analysis utilizing the Williamson-Hall plot (Figure 2), taking into account all of the diffraction peak, showed that the avg. crystallite size was a bit smaller at 5.57 nm. The measured crystallite size is smaller compared to values reported in previous studies [9, 10], which can be referred to the relatively low calcination temperature employed in this present work. Additionally, the positive slope of the W-H plot indicated the presence of tensile strain within the material. Lattice strain values, along with other crystallographic parameters, are summarized in Table 1. Using the X-ray diffraction data, the regions corresponding to the crystalline peaks and the amorphous region have been quantified to determine the degree of crystallinity and calculated to be 74.91%.

### *3.2. FESEM analysis*

The shape, morphology, and average particle size of the synthesized NPs were investigated using the FESEM. Using ImageJ software, the particles size distribution of $TiO_2$ NPs were evaluated. The FESEM micrograph (Figure 3) showing that the biosynthesized NPs are spherical in shape and uniformly dispersed. The size distribution histogram of $TiO_2$

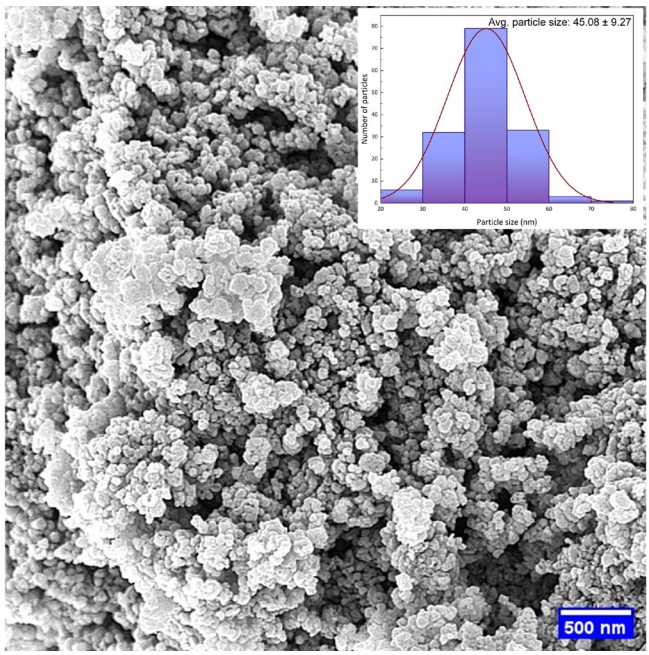


**Figure 3:** FESEM image of $TiO_2$ NPs and inset showing particle size distribution.

*https://doi.org/10.62275/josep.25.1000014*

NPs is shown in the inset of the same diagram, indicating that the majority of particles fall within the 30-60 nm range. The average particles size was found to be 45.08 nm. This nanoscale dimension is expected to enhance photocatalytic activity due to an increased surface-to-volume ratio [11].

### *3.3. Optical properties*

Investigating optical characteristics is essential for photocatalytic study because it provides information on the number of incident photons absorbed throughout the process [12]. Figure 4 shows the optical absorption spectra of $TiO_2$ NPs measured by a UV-vis spectrophotometer. The wavelength range where the intense absorptions were found was roughly 300–370 nm. $TiO_2$ nanoparticles light absorption properties were evaluated using UV-visible light having wavelengths between 300 and 800 nm. The observation revealed that ~361 nm was the absorption maxima of the $TiO_2$ nanostructures. The bandgap energy ($E_g$) of the $TiO_2$ nanostructures was calculated employing the Tauc plot, using the Eqn. 2 [13].

$$(\alpha h\upsilon)^2 = A(h\upsilon - E_g) \qquad (2)$$

where, $\alpha$ is absorbance coefficient, $h\upsilon$ is photon energy, $E_g$ is the bandgap energy, and $A$ is the equation constant. The calculated direct bandgap energy of the $TiO_2$ NPs was found to be 3.28 eV (inset of Fig. 4) and this closely aligns with the reported band gap value of 3.27 eV for bulk $TiO_2$ [14].

### *3.4. Photocatalytic activity evaluation*

$TiO_2$ nanoparticles are valued for photocatalytic activity due to their potent oxidizing ability, long-term stability, and lack of toxicity [15]. The photocatalytic performance of $TiO_2$ nanostructures strongly depends on particle size, surface area, crystallinity, and band gap [16]. Biosynthesis can enhance these by introducing unique surface modifications and morphology, improving light absorption and charge separation. In this study, using an organic dye (Methylene Blue) and solar light, the photocatalytic activity of biosynthesized $TiO_2$ NPs was demonstrated. The initial indication of dye degradation was observed through a color change. The dye displayed a characteristic visible light absorption spectrum, with its highest absorbance at 664 nm (Figure 5). This peak served as a reference for measuring and monitoring the dye concentration in the solution. From the absorbance spectra associated with dye degradation, it was clear that $TiO_2$ nanoparticles facilitated a steady rise in the

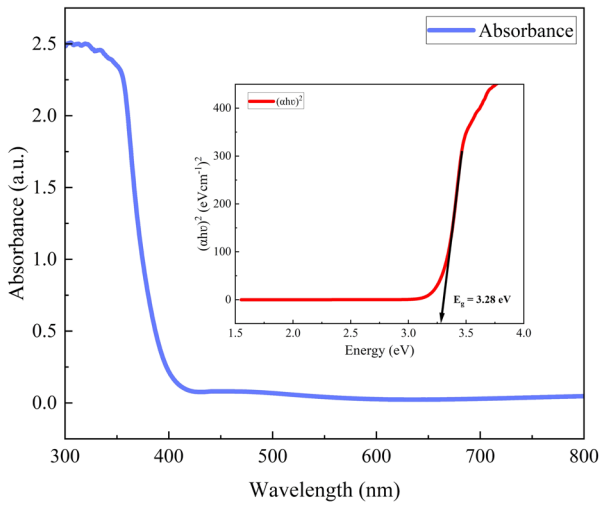


**Figure 4:** UV−vis absorption spectra, and inset showing the Tauc plot of $TiO_2$ NPs.

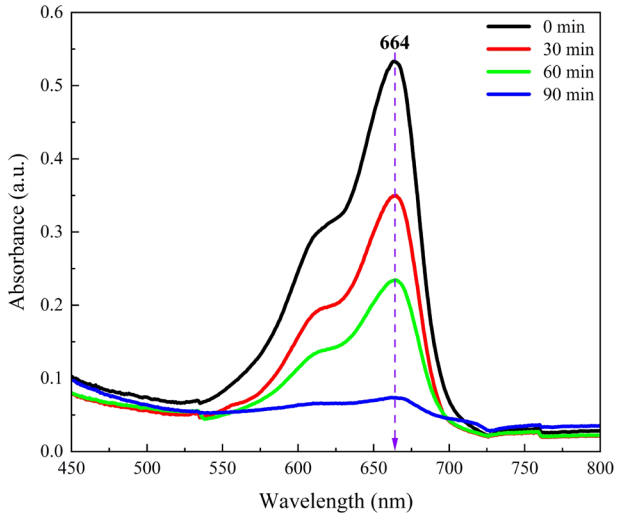


**Figure 5:** Absorption spectrum of $TiO_2$ NPs as a function of wavelength at 0, 30, 60, and 90 min.

percentage of dye degradation over time, demonstrated by the declining absorbance levels. Degradation rates for 30 and 60 min were found to be 34.59% and 56.02%, respectively. This finding signified that the percent deterioration increased with longer irradiation times and peaked at 86.23% after 90 minutes of solar irradiation. The amount of light energy impinging on the catalyst surface was absorbed as the irradiation time increased. Due to this, there was an increase in the generation of photo-excited species, which raised photocatalytic activity [17]. This investigation showed that increasing the exposure period improved the photocatalytic dye degradation process (Figure 5).

## 4. Conclusion

This study successfully employed garlic clove extract as a green reducing agent to fabricate zero-dimensional $TiO_2$ nanostructures. XRD analysis affirmed the formation of highly crystalline and pure anatase $TiO_2$ with sharp diffraction peaks and the absence of impurities. The synthesized NPs exhibited a uniform spherical morphology as revealed by FESEM imaging. UV-vis spectroscopy indicated a band gap energy comparable to bulk $TiO_2$. Significantly, the green synthesis method utilizing natural resources yielded $TiO_2$ with notable photocatalytic efficiency for degrading methylene blue under visible light exposure. This eco-friendly method holds potential for both dye effluent treatment and broader water purification applications.

## Reference

1. Shen, H. L., Hu, H. H., Liang, D. Y., Meng, H. L., Li, P. G., Tang, W. H., and Cui, C. (2012). Effect of calcination temperature on the microstructure, crystallinity and photocatalytic activity of $TiO_2$ hollow spheres. *Journal of Alloys and Compounds*, 542: 32–36.
2. Buraso, W., Lachom, V., Siriya, P., and Laokul, P. (2018). Synthesis of $TiO_2$ nanoparticles via a simple precipitation method and photocatalytic performance. *Materials Research Express*, 5(11): 115003.
3. Saranya, K. S., Vellora Thekkae Padil, V., Senan, C., Pilankatta, R., Saranya, K., George, B., Wacławek, S., and Černík, M. (2018). Green Synthesis of High Temperature Stable Anatase Titanium Dioxide Nanoparticles Using Gum Kondagogu: Characteri-

*https://doi.org/10.62275/josep.25.1000014*

zation and Solar Driven Photocatalytic Degradation of Organic Dye. *Nanomaterials*, 8(12): 1002.

4. Nabi, G., Ain, Q.-U.-, Tahir, M. B., Nadeem Riaz, K., Iqbal, T., Rafique, M., Hussain, S., Raza, W., Aslam, I., and Rizwan, M. (2022). Green synthesis of $TiO_2$ nanoparticles using lemon peel extract: their optical and photocatalytic properties. *International Journal of Environmental Analytical Chemistry*, 102(2): 434–442.
5. Chauhan, R., Kumar, A., and Chaudhary, R. P. (2012). Structural and photocatalytic studies of Mn doped $TiO_2$ nanoparticles. *Spectrochimica Acta Part A: Molecular and Biomolecular Spectroscopy*, 98: 256–264.
6. Ansari, A., Siddiqui, V. U., Rehman, W. U., Akram, Md. K., Siddiqi, W. A., Alosaimi, A. M., Hussein, M. A., and Rafatullah, M. (2022). Green Synthesis of $TiO_2$ Nanoparticles Using Acorus calamus Leaf Extract and Evaluating Its Photocatalytic and In Vitro Antimicrobial Activity. *Catalysts*, 12(2): 181.
7. Vijayakumar, S., Malaikozhundan, B., Saravanakumar, K., Durán-Lara, E. F., Wang, M.-H., and Vaseeharan, B. (2019). Garlic clove extract assisted silver nanoparticle – Antibacterial, antibiofilm, antihelminthic, anti-inflammatory, anticancer and ecotoxicity assessment. *Journal of Photochemistry and Photobiology B: Biology*, 198: 111558.
8. Anu, K., Singaravelu, G., Murugan, K., and Benelli, G. (2017). Green-Synthesis of Selenium Nanoparticles Using Garlic Cloves (Allium sativum): Biophysical Characterization and Cytotoxicity on Vero Cells. *Journal of Cluster Science*, 28(1): 551–563.
9. Moyeen, A. Al, Mahmud, R. M., Mazumder, D. D., Ghosh, S., Datta, O., Molla, A., and Begum, M. E. (2024). Investigation of structural, optical, antibacterial, and dielectric properties of sol-gel and biosynthesized $TiO_2$ nanoparticles. *Heliyon*, 10(23): e40776.
10. Sethy, N. K., Arif, Z., Mishra, P. K., and Kumar, P. (2020). Green synthesis of $TiO_2$ nanoparticles from Syzygium cumini extract for photo-catalytic removal of lead (Pb) in explosive industrial wastewater. *Green Processing and Synthesis*, 9(1): 171–181.
11. Le, N. T. H., Thanh, T. D., Pham, V.-T., Phan, T. L., Lam, V. D., Manh, D. H., Anh, T. X., Le, T. K. C., Thammajak, N., Hong, L. V., and Yu, S. C. (2016). Structure and high photocatalytic activity of (N, Ta)-doped $TiO_2$ nanoparticles. *Journal of Applied Physics*, 120(14): 142110.
12. Nabi, G., Majid, A., Riaz, A., Alharbi, T., Arshad Kamran, M., and Al-Habardi, M. (2021). Green synthesis of spherical $TiO_2$ nanoparticles using Citrus Limetta extract: Excellent photocatalytic water decontamination agent for RhB dye. *Inorganic Chemistry Communications*, 129: 108618.
13. Singh, M. K., and Mehata, M. S. (2019). Phase-dependent optical and photocatalytic performance of synthesized titanium dioxide ($TiO_2$) nanoparticles. *Optik*, 193: 163011.
14. Asahi, R., Morikawa, T., Ohwaki, T., Aoki, K., and Taga, Y. (2001). Visible-Light Photocatalysis in Nitrogen-Doped Titanium Oxides. *Science*, 293(5528): 269–271.
15. Ganesan, S., Babu, I. G., Mahendran, D., Arulselvi, P. I., Elangovan, N., Geetha, N., and Venkatachalam, P. (2016). Green engineering of titanium dioxide nanoparticles using Ageratina altissima (L.) King & H.E. Robines. medicinal plant aqueous leaf extracts for enhanced photocatalytic activity. *Annals of Phytomedicine : An International Journal*, 5(2): 69–75.
16. Thakur, N., Thakur, N., Kumar, A., Thakur, V. K., Kalia, S., Arya, V., Kumar, A., Kumar, S., and Kyzas, G. Z. (2024). A critical review on the recent trends of photocatalytic, antibacterial, antioxidant and nanohybrid applications of anatase and rutile $TiO_2$ nanoparticles. *Science of The Total Environment*, 914: 169815.
17. Saranya, K. S., Vellora Thekkae Padil, V., Senan, C., Pilankatta, R., Saranya, K., George, B., Wacławek, S., and Černík, M. (2018). Green Synthesis of High Temperature Stable Anatase Titanium Dioxide Nanoparticles Using Gum Kondagogu: Characterization and Solar Driven Photocatalytic Degradation of Organic Dye. *Nanomaterials*, 8(12): 1002.

**Funding**

The authors declare that no funds, grants, or other support were received during the preparation of this manuscript. The investigation was not funded by any organization or any sources.

**Acknowledgement**

The authors gratefully acknowledge the Department of Glass & Ceramic Engineering, Rajshahi University of Engineering & Technology, for providing access to the laboratory facilities that supported this research.

**Ethical Approval**

The submitted work is a unique contribution to the field, not published elsewhere in any form or language. Results are presented clearly, honestly, and without fabrication, falsification or inappropriate data manipulation (including image-based manipulation). Authors adhere to discipline-specific rules for acquiring, selecting and processing data.

**Consent of Participate**

The submitted work is experimental work performed in the laboratory. No human subject or living organism/tissue is involved in this research.

**Author Contributions**

All authors contributed to the study conception and design. Material preparation, data collection and analysis were performed by Raiyana Mashfiqua Mahmud, Abdullah Al Moyeen, and Abdul Al Mamun. The first draft of the manuscript was written by Raiyana Mashfiqua Mahmud and Abdullah Al Moyeen, and all authors commented on previous versions of the manuscript. All authors read and approved the final manuscript.

*https://doi.org/10.62275/josep.25.1000014*